

CONTENTS

CHAPTER 1	
PRINCIPLES OF ULTRASOUND	9
Introduction	10
Physics of Ultrasound	10
Ultrasound Image Formation	17
Role of the Pulse Generator and Nature of Ultrasound Pulses	19
The Transducer: Transmitter and Receiver	20
The Receiver: Signal Processing and Image Display	20
Image Construction and Depth Calculation	21
Grayscale Representation and Dynamic Range	21
Image Geometry: Scanning and Orientation	22
Management of the Main Controls: Time Gain Compensation, Gain, Acoustic Power, Focus, and Depth	22
Synthesis of the Final Image	24
Sequential Image Optimization Strategy	25
Echogenicity Terminology and Definitions: From Hypoechoic to Hyperechoic, with Practical Examples	26
Image Orientation and Nomenclature	30
Probe Movement Terminology and Optimization of Echo Detection	32
Ultrasound Acquisition Modes: A-mode, B-mode, M-mode, Doppler, and 3D/4D Imaging	32
Artifacts: Recognition and Management in Clinical Practice	36
Emerging Technologies: Contrast-Enhanced Ultrasound and Artificial Intelligence in Ultrasound	43
Conclusions	44
CHAPTER 2	
ULTRASOUND IMAGE ACQUISITION AND TISSUE IDENTIFICATION	53
Body Anatomical Planes and Probe Movements	54
Transducer Positioning and Spatial Orientation	56
Ultrasound Identification of Facial Tissues	57

CHAPTER 3	
ULTRASOUND IN AESTHETIC MEDICINE: TECHNICAL REQUIREMENTS	61
Device Selection: Technological Standards for Facial Aesthetic Ultrasound	62
Importance of High-Frequency Resolution	62
Transducer Selection and the Importance of Footprint	64
Technical Checklist for Optimal Facial Ultrasound Scanning	65
Relevance of Technological Progress and Guideline Adoption	65
CHAPTER 4	
ULTRASOUND ANATOMY OF THE FACE	67
4.1 FACIAL LAYERS: GENERAL CONSIDERATIONS	68
Overall Stratigraphic Organization of the Face	68
Skin	70
Superficial and Deep Fat	71
Facial Muscles and SMAS	74
Facial Vascularization	76
Facial Innervation	83
Salivary Glands	87
Conclusions	88
4.2 FOREHEAD AND GLABELLA	94
Layered Organization of the Forehead and Glabella	94
Skin and Subcutaneous Tissue	94
Frontalis Muscle	96
Superficial and Deep Fascial Layers of the Frontalis and Periosteum	96
Vascularization of the Forehead and Glabella	101
Innervation of the Forehead and Glabella	105
4.3 TEMPORAL REGION	110
Stratigraphic Organization of the Temporal Region	110
Vascularization of the Temporal Region	113
Innervation of the Temporal Region	119
Filler Injection Techniques in the Temporal Region: Approaches, Planes, and the Role of Ultrasound Guidance	121
Main Anatomical Risks of the Temporal Region	121
Safety and Prevention of Complications in the Temporal Region: the Fundamental Role of Ultrasound	122
4.4 PERIOCCULAR AND EYELID REGION	127
Stratigraphic Organization of the Periorcular and Eyelid Region	127
Tear Trough	130
Vascularization of the Periorcular Region and Tear Trough	135

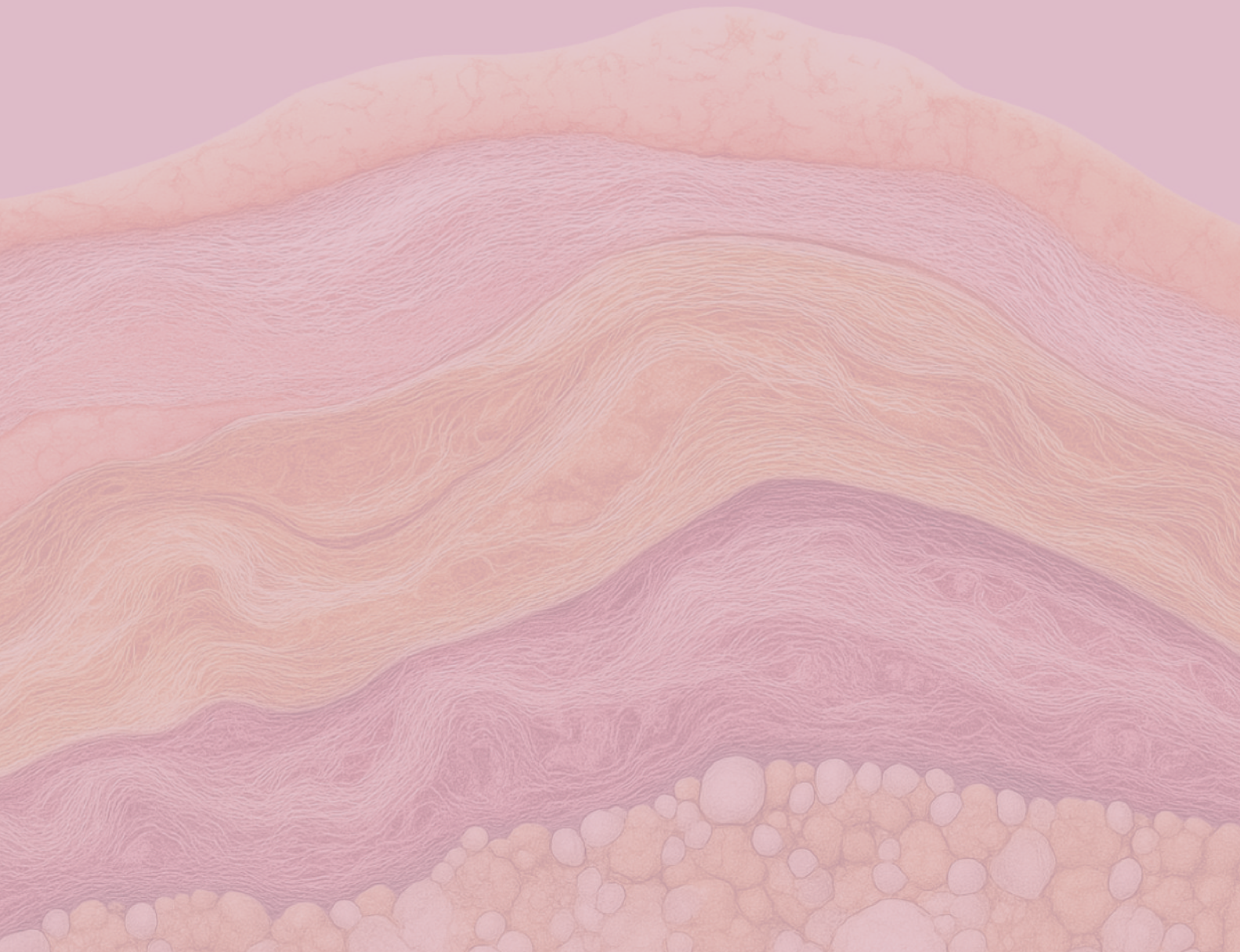
CONTENTS

4.5 NOSE	140
Introduction	140
Stratigraphic Organization of the Nose	140
Nasal Radix	143
Mid-Nasal Dorsum	144
Nasal Tip	145
Vascularization of the Nose	146
Conclusions	154
4.6 MALAR REGION	157
Introduction	157
Ultrasound Stratigraphy and Comparative Anatomical Complexity of the Malar, Zygomatic, and Infraorbital Regions	157
Fat Compartments and Retaining Ligaments of the Malar Region: Ultrasound Evaluation	165
Vascularization of the Malar Region	167
Clinical Considerations and Ultrasound Implications	169
4.7 CHEEK AND PREAURICULAR REGION	175
Introduction	175
Cheek (Genian Portion)	175
Preauricular Region	177
Arterial and Venous Vascularization of the Cheek and Preauricular Area	179
Innervation and Anatomical Risk Areas	181
Clinical Implications in Ultrasound-Guided Aesthetic Medicine	184
4.8 LIPS AND PERIORAL REGION	189
Introduction	189
Stratigraphic Organization of the Lips	189
Perioral Musculature	193
Arterial and Venous Vascularization of the Perioral Region	198
Innervation of the Perioral Region	201
Clinical Applications of Ultrasound in Perioral Aesthetic Treatments	203
4.9 CHIN AND MANDIBULAR REGION	212
Introduction	212
Stratigraphic Organization of the Chin and Mandible	213
Muscles of the Chin and Mandibular Region	214
Arterial and Venous Vascularization of the Chin and Mandibular Region	216
Innervation of the Chin and Mandibular Region	218

CHAPTER

1

PRINCIPLES OF ULTRASOUND



Introduction

Ultrasound imaging is based on a set of physical and technical principles that make it possible to obtain real-time images of tissues. This chapter provides a comprehensive overview of the fundamental concepts underlying ultrasound and represents an essential guide for clinicians who wish to use it competently in the field of aesthetic medicine. In particular, the chapter begins with the physics of ultrasound, analyzing the phenomenon of sound wave propagation through tissues and explaining how the frequency, amplitude, and intensity of the ultrasound beam influence image resolution and depth of penetration.

The process of ultrasound image formation is then described, illustrating the “pulse-echo” mechanism and the key role of piezoelectric crystals within the transducer. Particular emphasis is placed on parameter optimization, including gain, focus, and depth, which allow precise control of image brightness and sharpness. In parallel, the fundamental terminology used to describe tissue echogenicity (hypoechoic, hyperechoic, anechoic) is introduced, with practical examples aimed at establishing a shared diagnostic language.

The chapter then focuses on the most commonly used acquisition modes, ranging from B-mode, which is indispensable for two-dimensional grayscale imaging, to M-mode, used primarily in cardiology, and Doppler modalities (Color and Power Doppler) for the evaluation of vascular flow. Finally, the potential of 3D/4D technology is outlined, enabling volumetric reconstructions and real-time anatomical assessments.

A substantial section is devoted to ultrasound artifacts – inevitable phenomena that can alter image perception (such as acoustic shadowing, posterior acoustic enhancement, and mirror artifacts). Recognizing and managing these artifacts correctly is crucial to avoid diagnostic errors. Lastly, the chapter introduces emerging ultrasound technologies, including microbubble contrast-enhanced ultrasound and artificial intelligence, innovations that open exciting perspectives in aesthetic medicine by improving diagnostic quality and procedural safety.

Physics of Ultrasound

The physics of ultrasound constitutes the theoretical foundation upon which clinical ultrasound is based. A thorough understanding of these principles allows the physician to optimize image quality, correctly interpret visualized structures, and avoid diagnostic errors. Ultrasound consists of sound waves with frequencies above the threshold of human hearing, that is, greater than 20 kHz (Fig. 1). In diagnostic imaging, ultrasound probes typically operate at frequencies ranging from 1 to 20 MHz or higher, depending on clinical

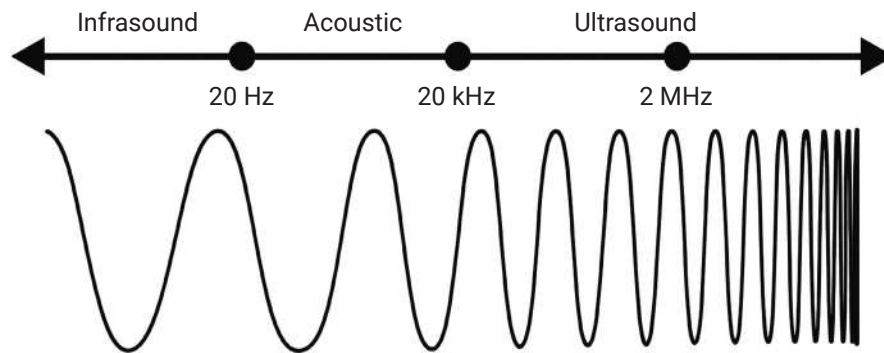


FIGURE 1
Sound wave spectrum

requirements and the anatomical region being examined.

For facial anatomy and its applications in aesthetic medicine, high frequencies – generally above 15 or 20 MHz – are preferred, as the need for spatial resolution is greater than that required for deeper examinations (such as abdominal imaging). However, it must always be borne in mind that increasing frequency reduces wave penetration, resulting in a shallower maximum imaging depth compared with lower-frequency probes.

As mechanical waves, ultrasound waves require a solid, liquid, or gaseous medium for propagation. In the human body, sound primarily traverses soft tissues and fluids, and to a lesser extent denser structures such as bone or cartilage, with varying efficiency depending on the physical properties of the tissue. Sound cannot propagate in a vacuum because, as a pressure wave, it requires molecules to undergo compression and rarefaction. The continuous alternation of compression and rarefaction zones represents the essence of a sound wave: during compression, molecules of the medium are pushed closer together, while during rarefaction they move apart, creating an oscillatory motion that travels along the direction of wave propagation (Fig. 2).

To analyze this phenomenon systematically, several acoustic parameters must be considered. Among the most important are frequency, period, wavelength, amplitude, power, and intensity (Fig. 3). Frequency, measured in hertz (Hz), indicates how many times a complete cycle (compression plus rarefaction) repeats in one second. A 1 Hz wave therefore completes one cycle per second, whereas a 1 MHz wave (one million Hz) completes one million cycles in the same time interval. The period is the mathematical inverse of frequency: if an ultrasound beam has a frequency of 10 MHz, its period will be 1/10,000,000 of a second. In practical terms, frequency and period provide information about how much “energy density” the wave carries over time and how this energy is distributed within tissues.

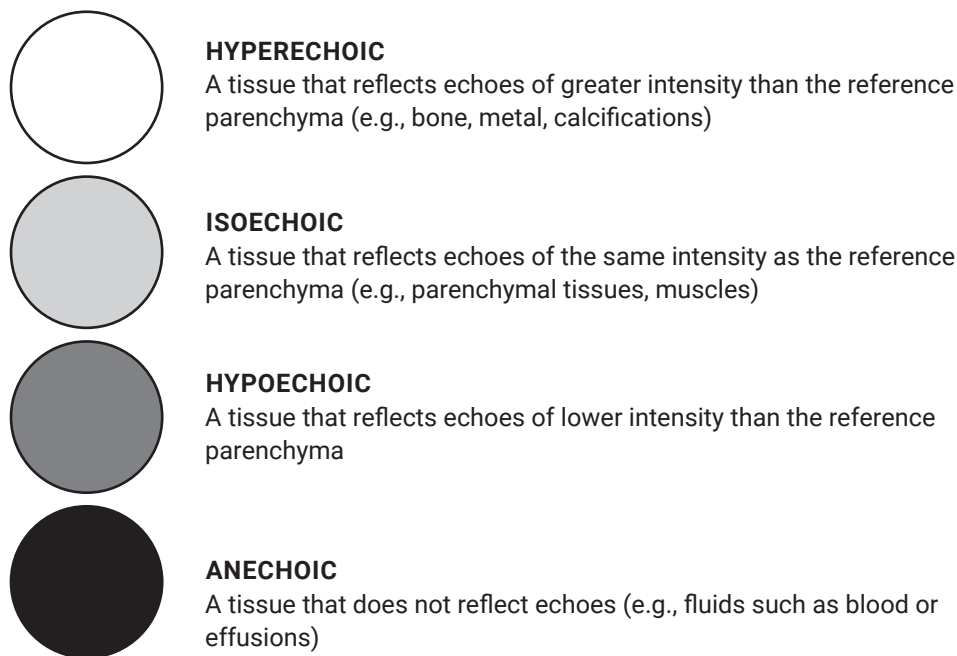


FIGURE 10
Echogenicity levels

to avoid misinterpreting the increased brightness as a pathological hyperechoic area.

- **Echotexture:** refers to the “pattern” or distribution of echoes within a tissue (fine or coarse, homogeneous or heterogeneous, reticular, etc.). For example, a tissue with uniform, small echoes may be described as having a “fine and homogeneous echotexture,” whereas a tissue with echoes of varying size and irregular distribution may be described as “coarse and heterogeneous”.

In these cases as well, terminology helps distinguish between physiological tissue (such as a fat pad) and altered tissue (such as a fluid collection or an area of fibrosis), as well as identify the presence of filler deposits or previously injected materials within their anatomical context.

When using terms such as hypoechoic, hyperechoic, anechoic, or isoechoic, the comparison is always made relative to a reference tissue. In the literature, hepatic parenchyma is often used as a standard reference in abdominal ultrasound. In the facial region, a practical example would be comparing a filler deposit with the adjacent adipose tissue: if the filler appears darker, it would be described as hypoechoic relative to fat (even though fat itself may be considered hypoechoic relative to muscle). It is therefore essential to explicitly state the reference tissue used for comparison.

Although the hypoechoic/isoechoic/hyperechoic nomenclature is extremely useful,

FACIAL LAYERING

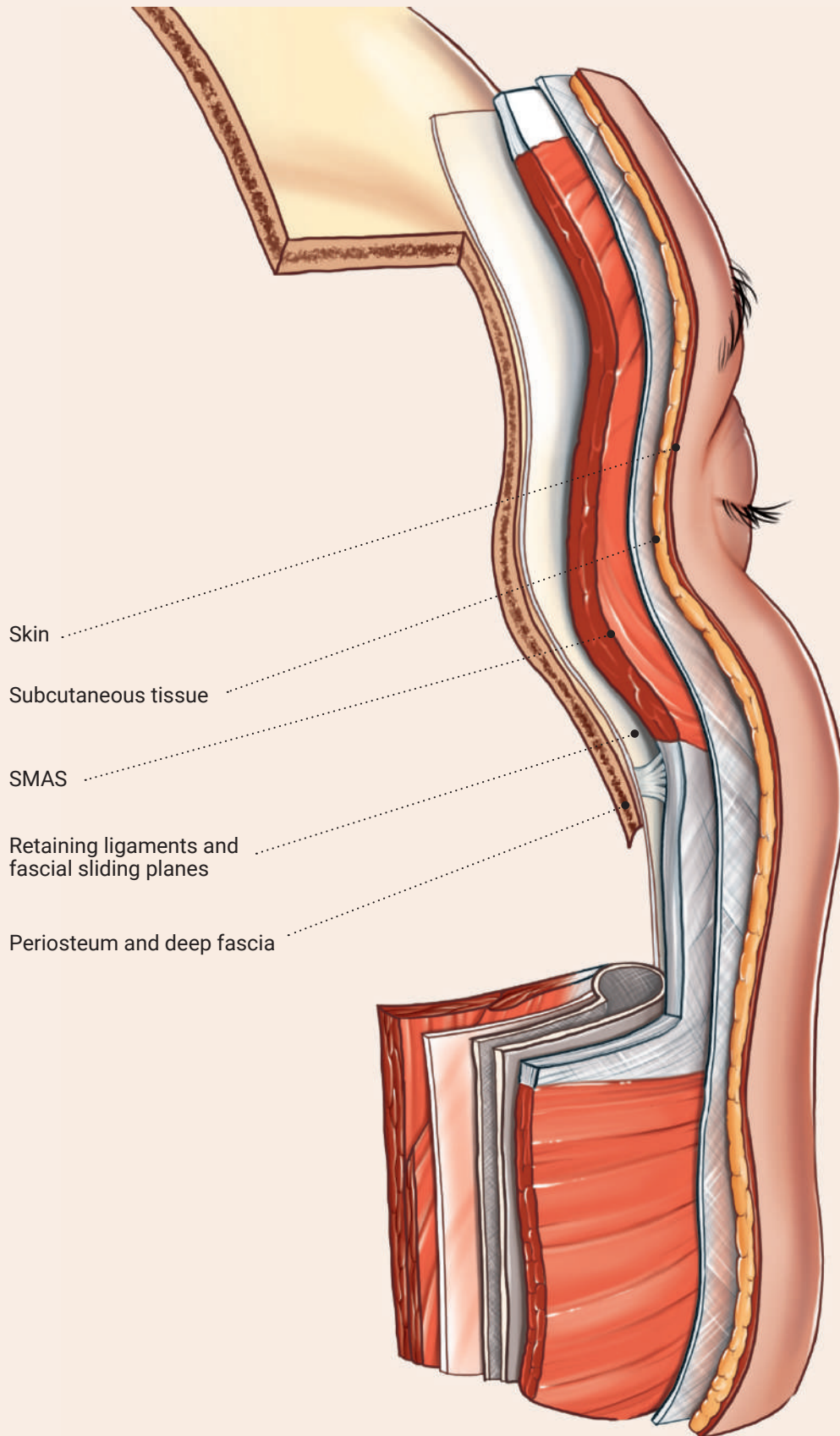
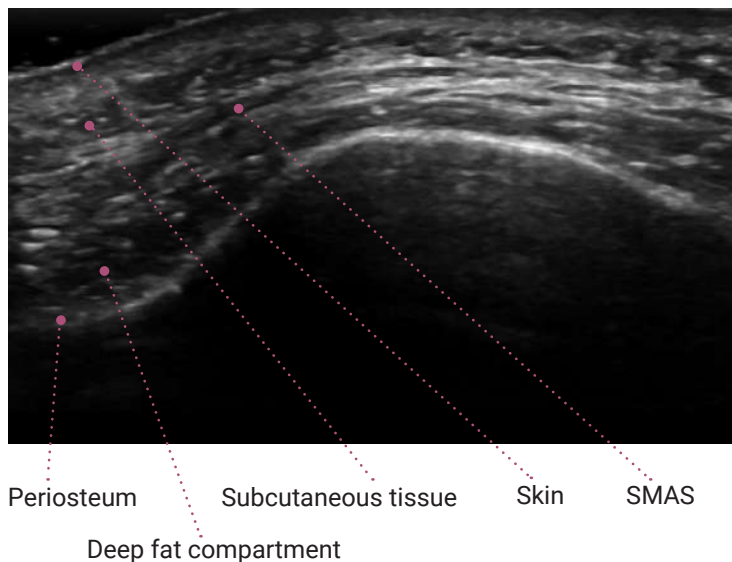


FIGURE 27
Anatomical illustration of the facial layers in sagittal and medial transverse view

**FIGURE 28**

Ultrasound image, transverse scan at the zygomatic level, showing the five fundamental layers

This organization may be altered by the presence of glandular structures (parotid gland, minor salivary glands), major vessels or nerves, or ligamentous insertions that interrupt the continuity of fat compartments.

Ultrasound scanning should always follow this layered logic, aiming to align the observed planes with their anatomical counterparts. Layering can vary significantly between facial regions, from thin and simple areas (e.g., tear trough or nasal dorsum with three layers) to thick and complex ones (e.g., the temple, with up to ten identifiable layers).

Skin

The skin forms the most superficial covering and comprises the epidermis and dermis. Sonographically, it appears as a superficial hyperechoic band, with a thin hyper-reflective line (epidermis) overlying a band of intermediate echogenicity (dermis).

Cutaneous thickness varies markedly by region, as confirmed by Kim et al. and both ultrasound and histologic studies:

- **eyelid and periorbital areas**, thinnest skin (0.4-0.8 mm);
- **nasal, mental, and zygomatic areas**, thicker skin (1.5-2 mm).

This variability has direct clinical implications: injection depth must be adapted to skin thickness and elasticity to avoid overcorrection, nodules, or product visibility in thin regions.

SUPERFICIAL FACIAL FAT COMPARTMENTS

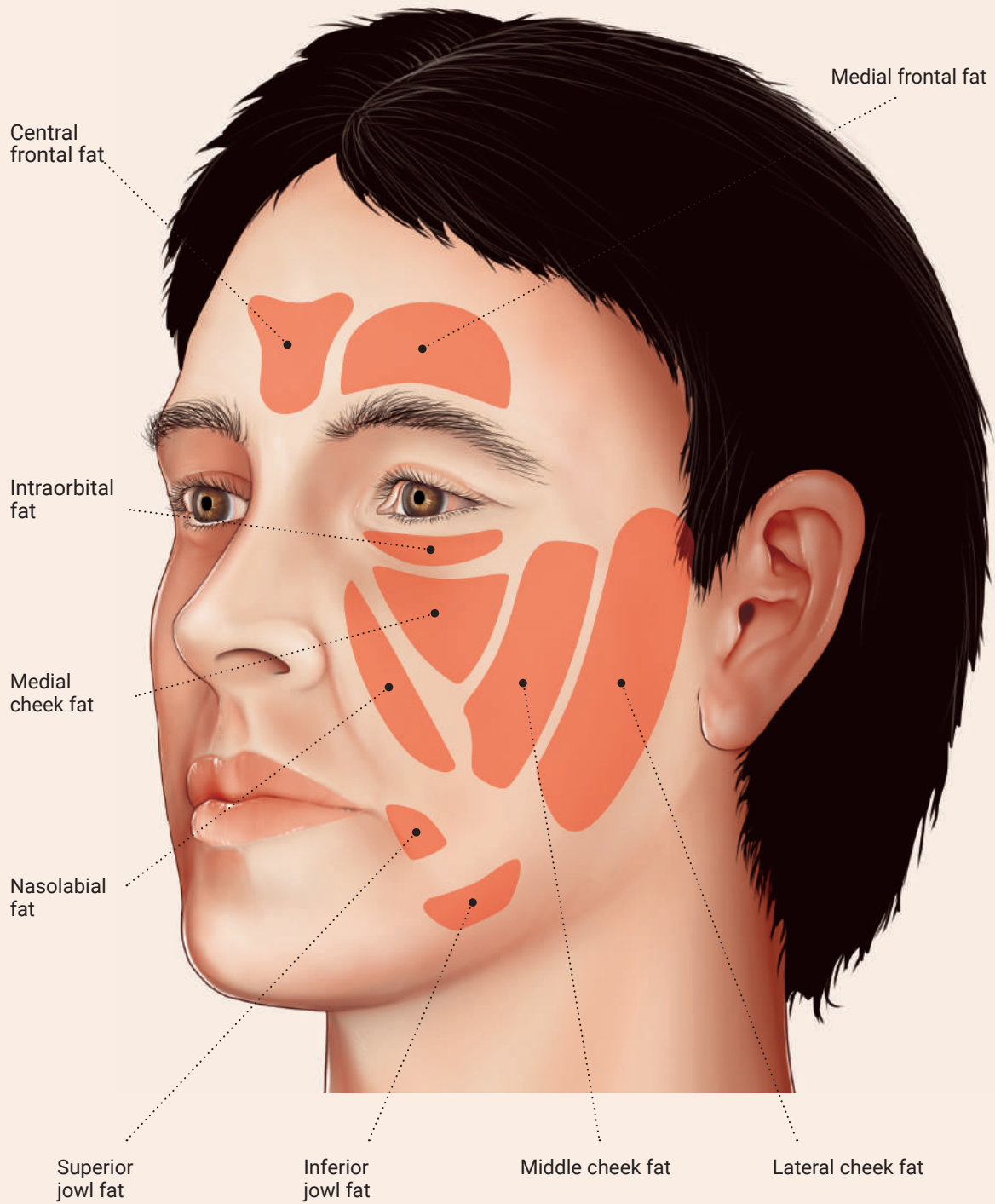


FIGURE 29A

Illustrative drawing of facial fat compartmentalization: superficial fat compartments

id artery, which emerges at the inferior mandibular border and ascends along the cheek medial to the masseter.

Major branches include:

- **inferior labial artery;**
- **superior labial artery;**
- **submental artery;**
- **lateral nasal artery;**
- **angular artery.**

The facial artery typically terminates as the angular artery, which travels toward the medial canthus and may anastomose with branches of the ophthalmic artery, such as the dorsal nasal and supratrochlear arteries – creating potential pathways for retrograde embolization and complications such as necrosis and blindness.

Another key vessel is the superficial temporal artery (STA), a terminal branch of the external carotid. It emerges anterior to the tragus, runs within the superficial temporal fascia, and divides into frontal and parietal branches. The frontal branch courses anterosuperiorly toward the forehead, often along the temporal line, and is particularly relevant during injections in the temporal and frontal regions due to its variable depth and vulnerability.

Ultrasound and cadaveric studies have shown wide variability in STA depth, which may be subcutaneous, interfascial, or subfascial. Because of this variability and proximity to the temporal branch of the facial nerve, routine Doppler ultrasound is justified for precise localization.

Facial Artery, Angular Artery, and Anatomical Variants: Implications for Ultrasound-Guided Aesthetic Medicine

The facial artery, a terminal branch of the external carotid, is the major vessel supplying the central and lower face. Its course is tortuous and superficial: emerging at the mandibular border near the anterior masseter, crossing the mandible, ascending diagonally along the cheek, traversing the nasolabial fold, and terminating near the medial orbital region as the angular artery.

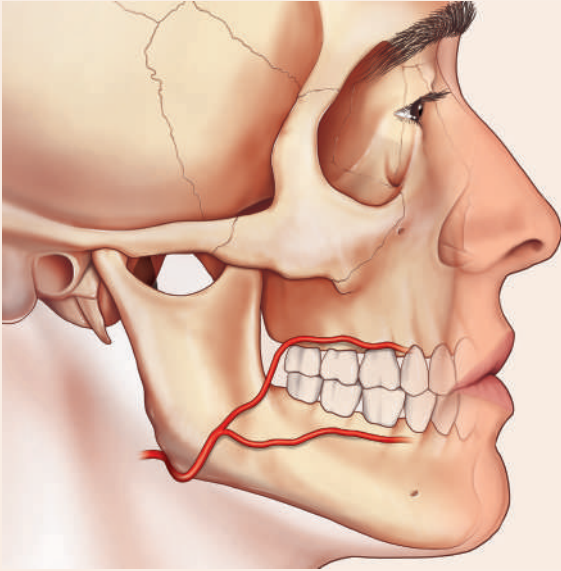
During its course it gives rise to branches such as the superior and inferior labial arteries, the lateral nasal artery, and occasionally the columellar artery. According to Koziej et al. (2022):

- the superior labial artery is present in 82.2% of cases;
- the angular artery in 42.5%, confirming high variability.

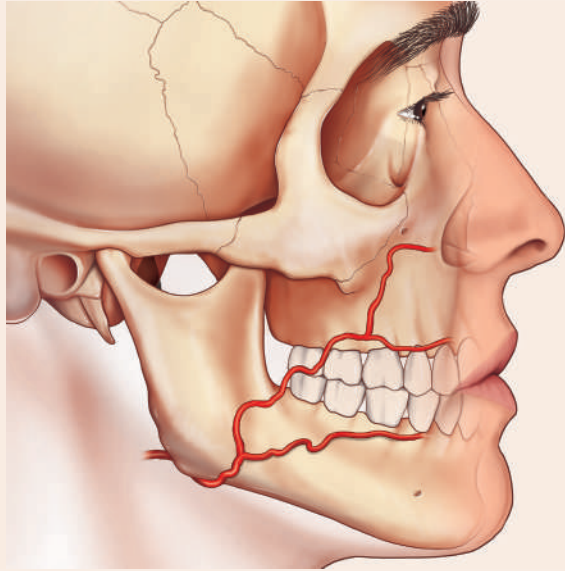
The angular artery may arise not only from the facial artery but also from the ophthalmic artery, infraorbital artery, or transverse facial artery (variant type V). Furukawa's classification, referenced by Koziej, describes five distinct patterns of facial artery course (Fig. 32).

FACIAL ARTERY COURSE: ANATOMICAL VARIANTS

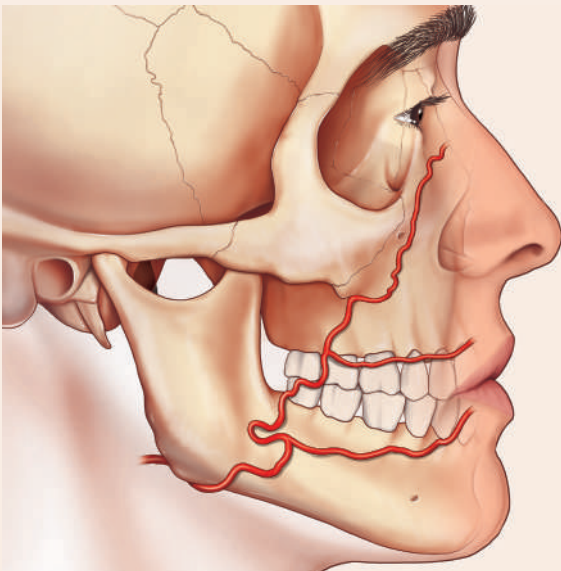
TYPE I - 24,7%



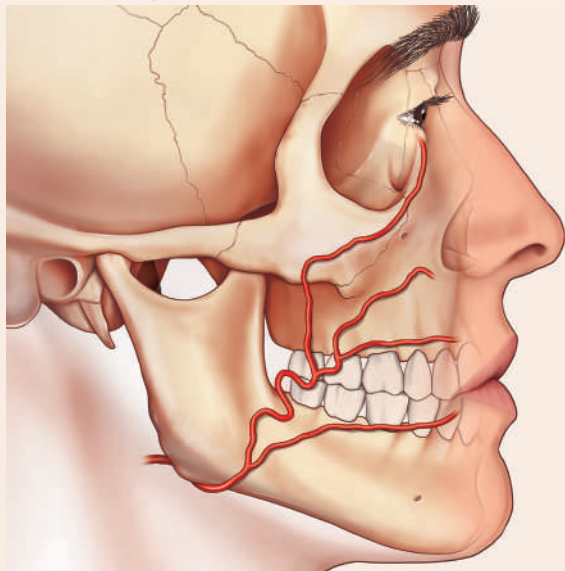
TYPE II - 31,4%



TYPE III - 40%



TYPE IV - 1,6%



TYPE V - 2,4%

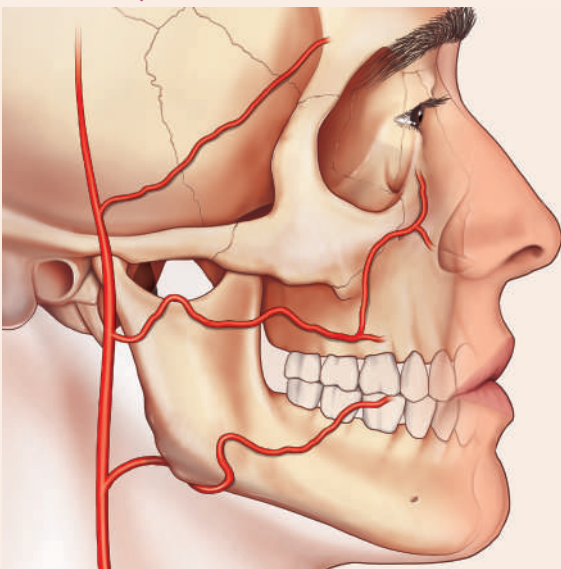


FIGURE 32

Facial artery classification by types and their occurrence

Type I: terminates proximal to the superior labial artery.

Type II: terminates distal to the superior labial artery, close to the nasolabial fold.

Type III: textbook course, lateral nasal or angular artery as the final branch.

Type IV: duplex with a dominant lateral angular branch.

Type V: additional type of facial artery course, where the vessel is hypoplastic and the remaining course is supplied by the dominant transverse facial artery.

4.2

FOREHEAD AND GLABELLA

Layered Organization of the Forehead and Glabella

Ultrasound examination of the frontal region represents one of the most significant steps in facial imaging in aesthetic medicine, as it allows real-time assessment of an area that is topographically simple yet rich in anatomically, functionally, and clinically relevant structures. Although the forehead is one of the most linear facial regions morphologically, it is characterized by complex tissue stratification, with variations in thickness, density, and composition across its upper, middle, and lower thirds, as well as the presence of neurovascular structures whose position may vary considerably among individuals.

Skin and Subcutaneous Tissue

The frontal skin appears on ultrasound as a two-layered structure: the epidermis, seen as a linear hyperechoic band, and the dermis, less reflective and appearing as an intermediate layer with variable echogenicity depending on collagen content and hydration levels. Its mean thickness is approximately 1.7-2.0 mm in the upper third, progressively decreasing to 1.5-1.7 mm in the middle third and to values below 1.4 mm in the glabellar region. Individual variability is influenced by sex, age, and BMI.

Immediately beneath the dermis lies the superficial fat layer, which appears as a hypoechoic band interrupted by hyperechoic fibrous septa. Superficial frontal fat exhibits high variability in thickness: it is more represented in the upper third (up to 4.0 mm), becomes thinner in the middle third (2.0-2.5 mm), and may be nearly absent in the glabella, where it is replaced by dense, minimally deformable fibroadipose tissue, often adherent to the underlying muscle (Fig. 37).

FIGURE 37

Longitudinal scan of the forehead along the hemipupillary line, with an anatomical illustration of the tissue layers of the frontal region

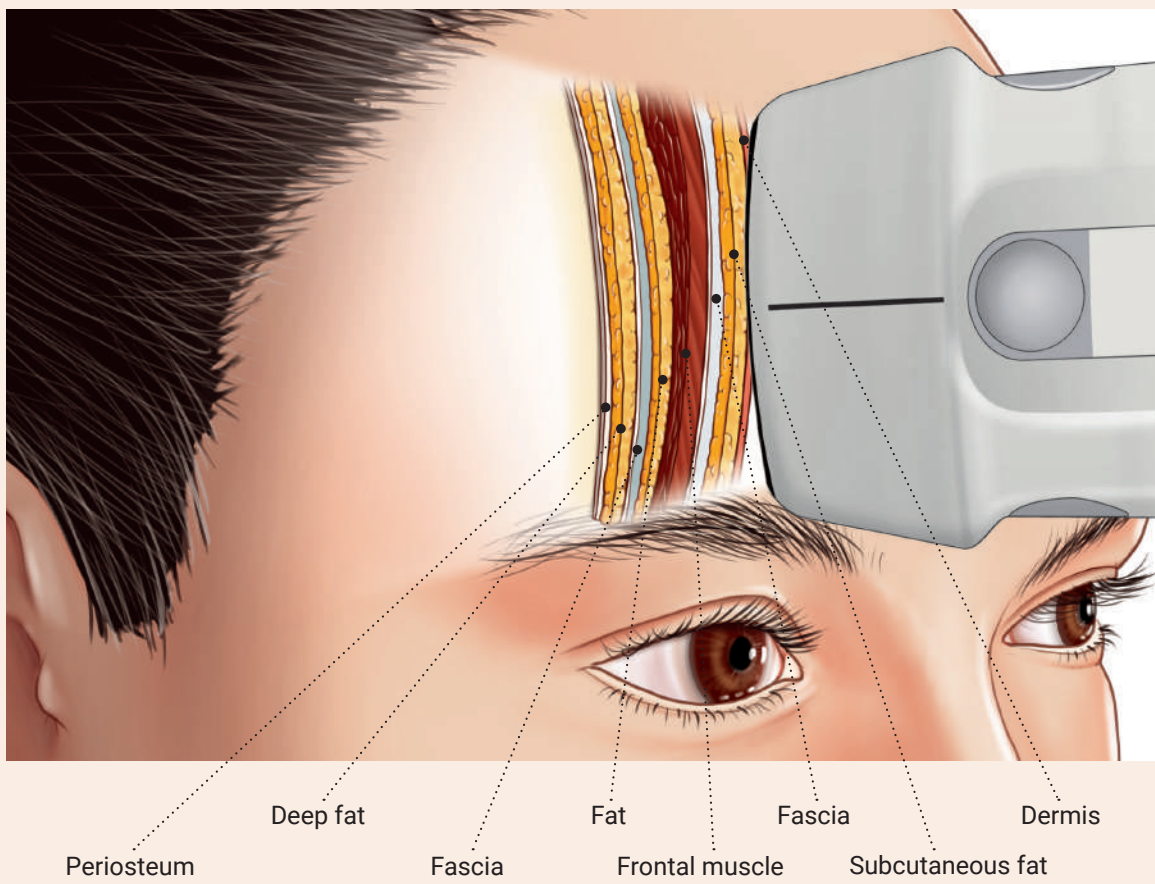
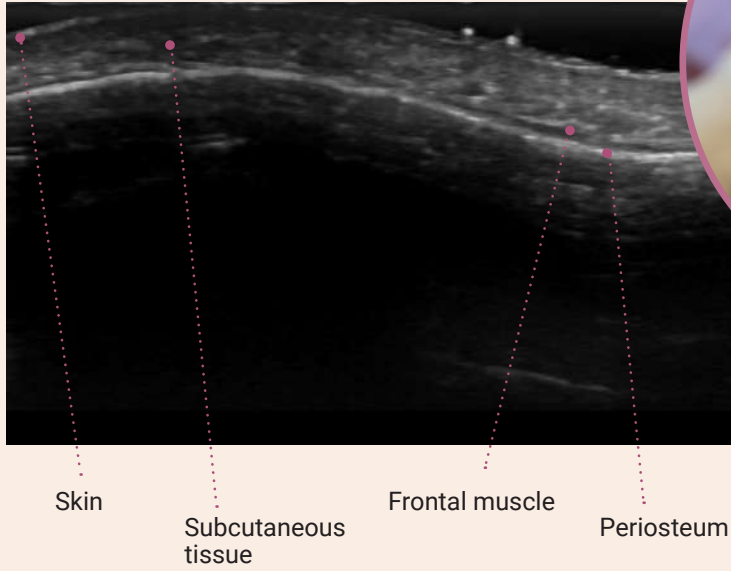


FIGURE 39A

Transverse scan of the median glabella showing the procerus, corrugator supercilii, and orbicularis oculi muscles, alongside an anatomical illustration of the glabellar musculature

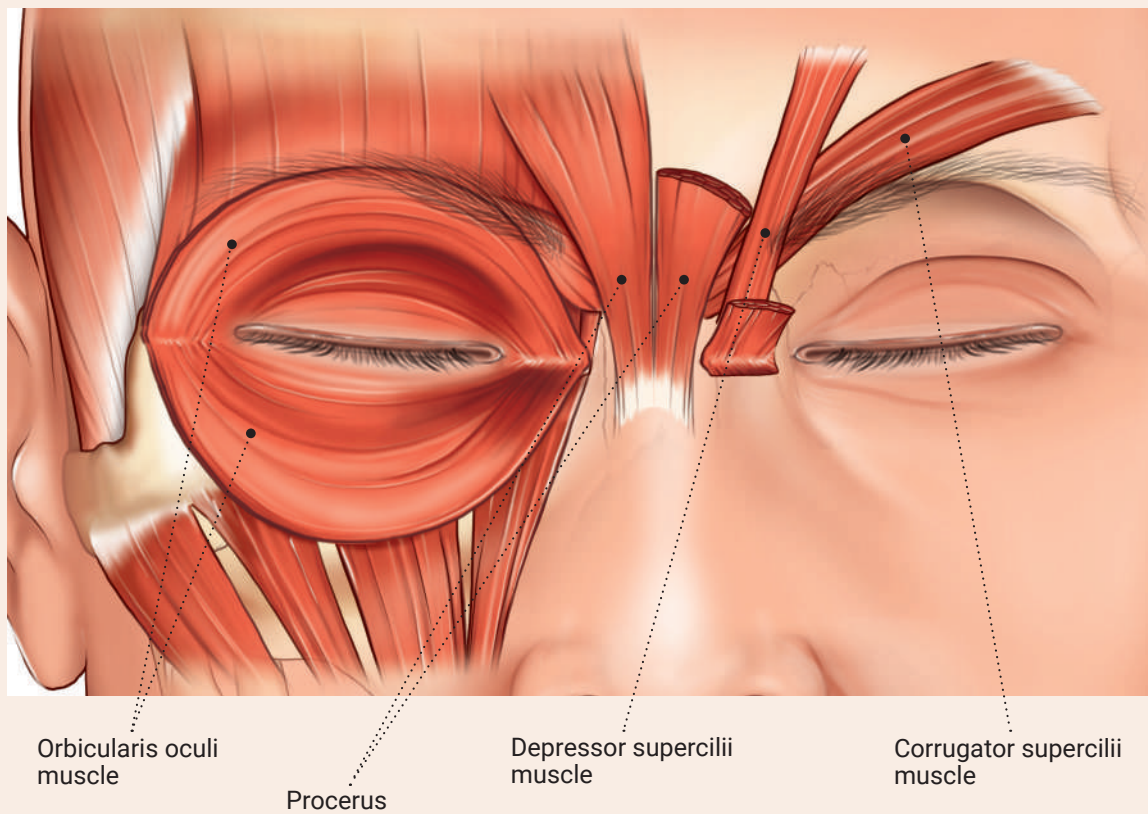
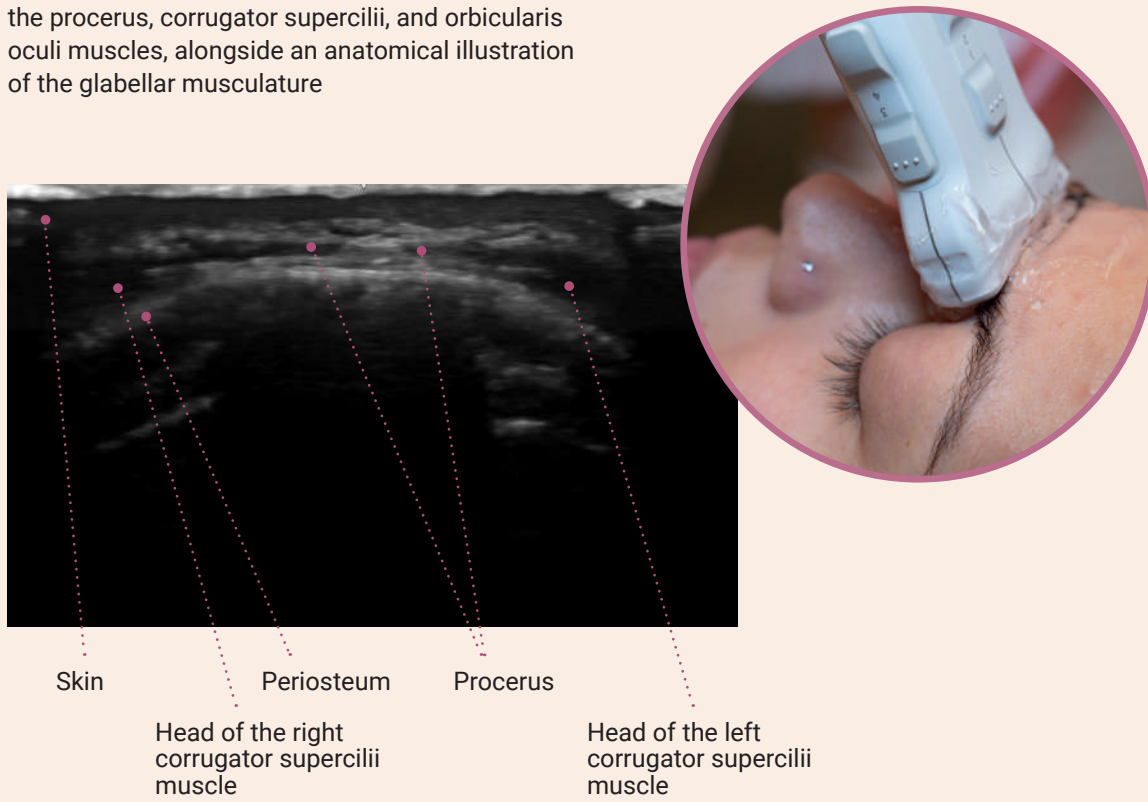
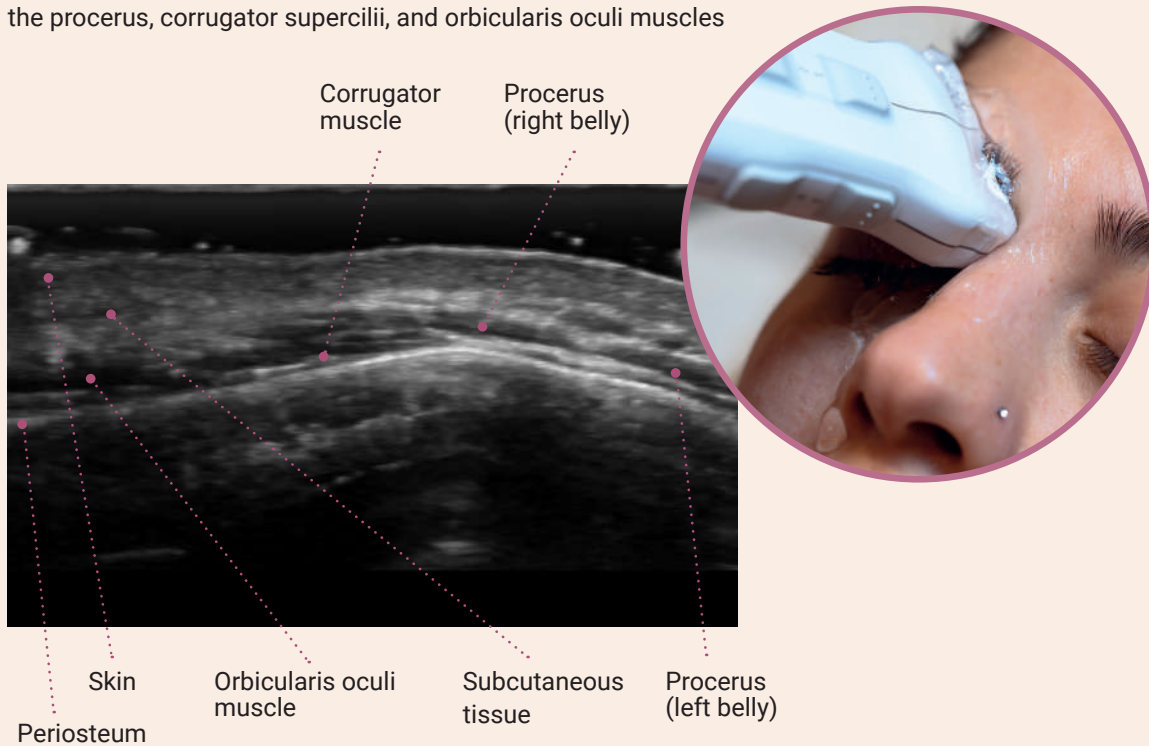


FIGURE 39B

Transverse scan of the paramedian glabella showing the procerus, corrugator supercilii, and orbicularis oculi muscles



The procerus muscle occupies the midline of the glabella, lying superficially to the nasal bone and periosteum. It originates from the upper portion of the lateral nasal cartilage and nasal bone, inserting into the dermis between the eyebrows. Functionally, it depresses the medial eyebrows, producing transverse nasion lines.

On ultrasound, it appears as a small triangular hypoechoic structure, originating on the nasal bone periosteum and inserting into the midline glabellar skin. In some individuals, it is composed of two paramedian muscle bellies forming a “V” shape. Mean thickness is 1.0-1.5 mm, and its surface is closely related to the supratrochlear artery, which may cross or pass superficial to it. Optimal visualization requires high-frequency probes and sufficient gel to avoid compression of superficial layers.

The procerus is a key target for botulinum toxin in treating glabellar lines. Literature reports a mean supratrochlear artery depth of 2.2-4.4 mm at this level, with considerable variation by sex and tissue thickness (Fig. 40).

STRATIFICATION OF THE NOSE

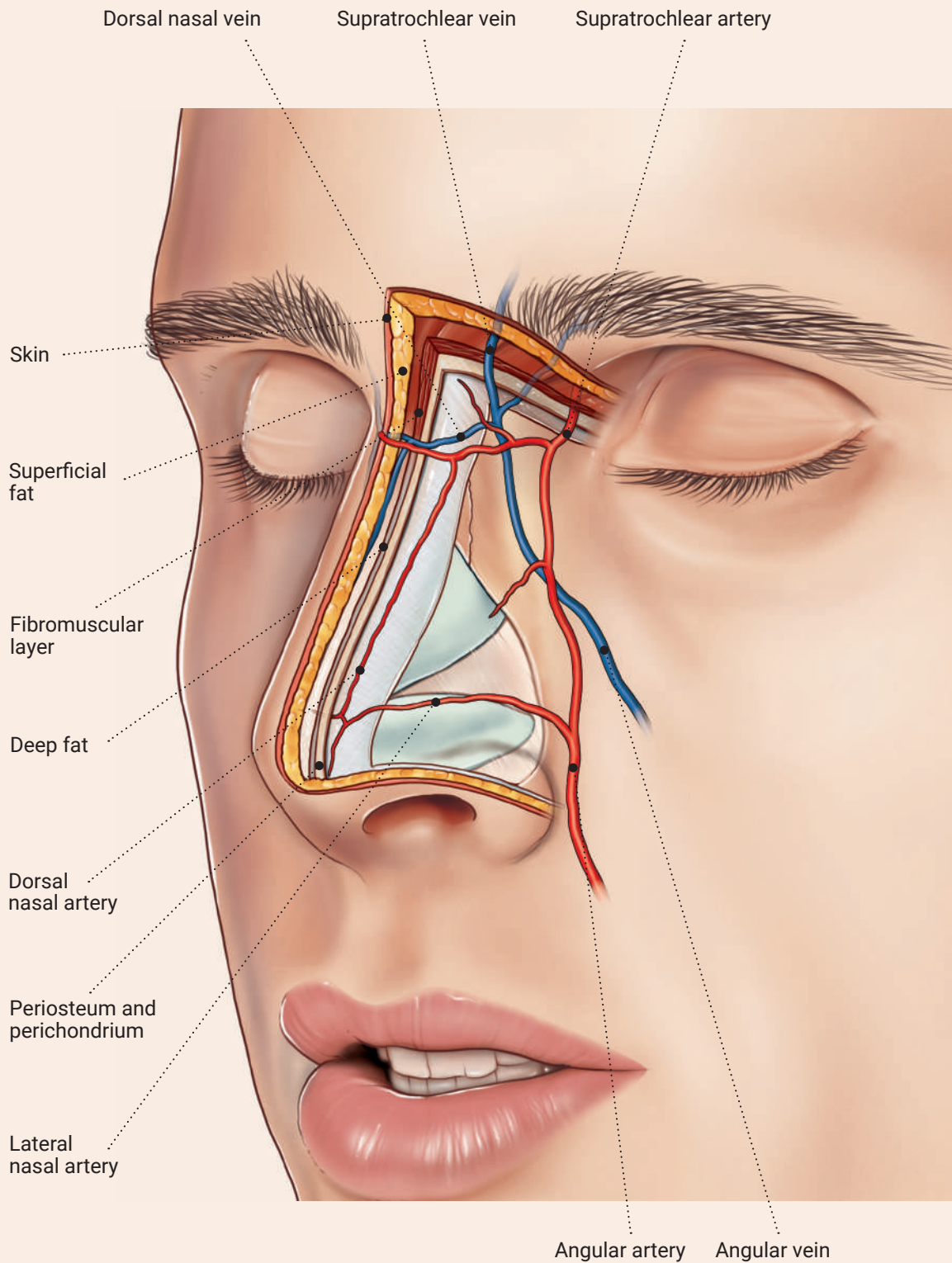


FIGURE 59B

Anatomical drawing of the tissue layer stratification at the level of the nose and the corresponding arterial and venous vascularization

Nasal Radix

The nasal radix extends from the glabella to the transition point with the nasal bones. On ultrasound, the radix shows a simplified stratification, in which the following structures can be identified (Fig. 60):

1. **Skin (epidermis and dermis):** hyperechoic layer of moderate thickness.
2. **Thin subdermal adipose layer:** often <1 mm, poorly developed.
3. **Procerus muscle:** hypoechoic, vertically oriented
4. **Nasal bone:** deep hyperechoic margin with posterior acoustic shadowing.

In this region, the muscular component predominates, with direct insertion of the procerus muscle onto bone. No deep adipose layer is present. The dorsal nasal artery typically courses superficially, within the subdermal adipose tissue.

FIGURE 60A

Transverse scan of the nasal root and the proximal third of the nasal dorsum

